

doi: 10.3969/j.issn.0490-6756.2020.05.016

# 相关噪声驱动下一种特殊非对称 非线性系统的随机共振研究

范泽宁<sup>1</sup>, 李鹏飞<sup>1</sup>, 陶原野<sup>2</sup>, 唐一弓<sup>3</sup>, 邓科<sup>1</sup>

(1. 四川大学数学学院, 成都 610065; 2. 平安银行股份有限公司博士后工作站, 深圳 518000;  
3. 四川大学生命科学学院, 成都 610065)

**摘要:** 本文分析了在乘性非高斯噪声与加性高斯噪声驱动下的一种特殊非对称双稳系统的随机共振现象。我们使用统一色噪声逼近、路径积分法、二态模型理论对本文郎之万方程进行马尔科夫逼近, 从而得到系统的稳态概率分布与信噪比。仿真结果得知, 非高斯噪声与高斯噪声强度驱动下的信噪比均存在随机共振, 且非高斯噪声偏差参数、噪声相关时间、非对称系数、互相关强度等参数均对其有影响。本文分别讨论了非高斯噪声偏差参数, 非高斯噪声的相关时间, 互相关强度, 周期信号幅度和非对称系数等参数对信噪比的影响。

**关键词:** 随机共振; 非对称双稳系统; 福克-普朗克方程; 稳态概率分布; 信噪比

**中图分类号:** O414.21      **文献标识码:** A      **文章编号:** 0490-6756(2020)05-0927-09

## Stochastic resonance in a special type of asymmetric nonlinear system driven by correlated noise

FAN Ze-Ning<sup>1</sup>, LI Peng-Fei<sup>1</sup>, TAO Yuan-Ye<sup>2</sup>, TANG Yi-Gong<sup>3</sup>, DENG Ke<sup>1</sup>

(1. College of Mathematics, Sichuan University, Chengdu 610065, China;  
2. Ping An Bank Co., Ltd., Shenzhen 518000, China;  
3. College of Life Sciences, Sichuan University, Chengdu 610065, China)

**Abstract:** We have analyzed the phenomenon of stochastic resonance in an asymmetric bistable system driven by multiplicative non-Gaussian noise and additive Gaussian noise. Using a path-integral approach, together with the unified colored noise approximation and two-state model theory, we have obtained a consistent Markovian approximation, which enables us to get the analytical expressions for the stationary probability distribution and the signal-to-noise ratio. Under the influence of non-Gaussian noise deviation parameter, noise correlation time, asymmetric coefficient and mutual correlation strength, there are stochastic resonance on signal-to-noise ratio as non-Gaussian noise intensity and Gaussian noise intensity. Besides, the influence of different parameters on signal-to-noise ratio is discussed respectively, including non-Gaussian noise deviation parameter, correlation times of the non-Gaussian noise, cross-correlation strengths, amplitudes of periodic signal, and asymmetric coefficient.

**Keywords:** Stochastic resonance; Asymmetric bistable system; Fokker-Planck equation; Stationary probability distribution; Signal-to-noise ratio

收稿日期: 2019-04-23

基金项目: 中央高校基本科研基金(2682018CX65); 国家自然科学基金青年基金(11301361)

作者简介: 范泽宁(1993-), 女, 山西大同人, 博士研究生, 研究方向为非线性动力系统与统计物理学. E-mail: zeningfan@126.com

通讯作者: 邓科. E-mail: dk\_83@126.com

## 1 Introduction

The original work on stochastic resonance by Benzi *et al.*<sup>[1]</sup> in 1981, in which the term was coined, was in the context of modeling the switching of the Earth's climate between ice ages and periods of relative warmth with a period of about 100 000 years. From 1983 to 1989, Pesquera *et al.*<sup>[2-3]</sup> analyzed this type of non-Markovian processes in terms of a path integral formulation is rare up to recent times. In 1989, Presilla *et al.*<sup>[4]</sup> came up with the famous adiabatic approximation theory successively. From 1989 to 1991, adiabatic perturbation theory was put forward by Jung and Hanggi<sup>[5-6]</sup>, that provides a necessary theoretical basis for the study of stochastic resonance. At the present stage, the study of stochastic resonance under complex system and complex noises is helpful to feature extraction and detecting weak signal of high-precision machinery at low SNR situation<sup>[7-9]</sup>.

Up to now, there are many theoretical studies on resonance stochastic. Moreover, there are many studies on symmetric bistable potential function systems<sup>[10]</sup>. But it turns out that asymmetric systems can be used in many physical contexts<sup>[11]</sup> for the past few years, just as the mechanical model of the harmonic oscillators<sup>[12]</sup>, the external magnetic field the energy acquisition system of a cantilever beam<sup>[13]</sup>, the superconducting quantum interference devices to detect weak signals<sup>[14-15]</sup>, *etc.* Besides, there are many researches on stochastic resonance in asymmetric systems. Zhou *et al.*<sup>[16]</sup> studied stochastic resonance in an asymmetric bistable system driven by trichotomous noises, Jiao *et al.*<sup>[17]</sup> studied stochastic resonance of asymmetric bistable system with alpha stable noise.

On the other hand, in almost cases, the noises are assumed to be Gaussian. However, some experimental results in sensory systems, the noise source in some systems could be non Gaussian<sup>[18-19]</sup>. Therefore, some scholars have studied the stochastic resonance of the non-gaussian

case<sup>[20-21]</sup>. Fuentes *et al.*<sup>[22]</sup> use an effective Markovian approximation, path integral approach method, to simplify non-Gaussian noise. Guo *et al.*<sup>[10, 23]</sup> investigated symmetry bistable system and FitzHugh - Nagumo neural system driven by non-Gaussian noise. Shi *et al.*<sup>[24]</sup> investigated stochastic resonance in a special kind of asymmetric system.

The summary of contents and main results of this paper are as follows. We study the stochastic resonance phenomenon in an asymmetric nonlinear system driven by the non-Gaussian noise. In Section 2, using a path-integral approach, the unified colored noise approximation and the two-state model theory, we obtain the Fokker-Planck equation of the asymmetric bistable system and the analytical expressions for steady-state probability density function. In Section 3, the analytical expression of signal-to-noise ratio of asymmetric bistable systems with weak periodic signals is derived. And the influence of different parameters on SNR is discussed, including non-Gaussian noise deviation parameter, correlation times of the non-Gaussian noise, cross-correlation strengths, amplitudes of periodic signal, asymmetric coefficient, and both Gaussian and non-Gaussian noise intensities. And the conclusions drawn are summarized in Section 4.

## 2 PDF of a special type of asymmetric bistable system

We consider a special type of asymmetric bistable SR system driven by correlated additive and multiplicative non-Gaussian noise and its Langevin equation has been obtained as below:

$$\frac{dx}{dt} = -\frac{dU(x)}{dx} + A\cos(\Omega t) + x(t)\eta(t) + \xi(t) \quad (1)$$

where  $A\cos(\Omega t)$  is a periodic signal,  $A$  and  $\Omega$  are the amplitude and frequency of the periodic signal.  $U(x)$  is the asymmetric bistable potential function based on Refs. [24-25], and it can be written as below:

$$U(x) = -\frac{a}{2}x^2 + \frac{r}{3}x^3 + \frac{b}{4}x^4 \quad (2)$$

in which,  $a$  and  $b$  are the potential parameters, and  $r$  denotes the asymmetry of the potential. When  $r=0$ , the potential function  $U(x)$  reduces to that of a symmetric bistable system.

Fig. 1 shows the potential function as a function of  $x$  with different asymmetric parameters  $r$ . It is observed that as  $r$  is increased, the depth of the left potential well also gradually increases.

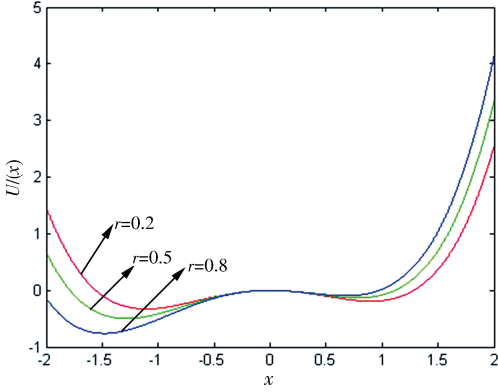


Fig. 1 The asymmetric bistable potential for different parameters  $r$  when  $a=1$  and  $b=1$

According to Eq. (2), we can obtain two stable states  $x_{s1}, x_{s2}$  and an unstable state  $x_{un}$  by solving  $dU(x)/dx=0$ .

$$\begin{aligned} x_{s1} &= \frac{-r - \sqrt{r^2 + 4ab}}{2b} \\ x_{s2} &= \frac{-r + \sqrt{r^2 + 4ab}}{2b} \\ x_{un} &= 0 \end{aligned} \quad (3)$$

The multiplicative noise term  $\eta(t)$  in system (1) has a non-Gaussian distribution<sup>[20, 22-23]</sup>.

$$\frac{d\eta(t)}{dt} = -\frac{1}{\tau} \frac{d}{d\eta} V_q(\eta) + \frac{1}{\tau} \epsilon(t) \quad (4)$$

in which,

$$\begin{aligned} V_q(\eta) &= \frac{D}{\tau(q-1)} \ln \left[ 1 + \frac{\tau(q-1)\eta^2}{D} \right] \\ \langle \eta(t) \rangle &= 0 \\ \langle \eta^2(t) \rangle &= \begin{cases} \frac{2D}{\tau(5-3q)}, & q \in \left( -\infty, \frac{5}{3} \right) \\ \infty, & q \in \left( \frac{5}{3}, 3 \right) \end{cases} \end{aligned} \quad (5)$$

By changing a single parameter  $q$ , we can control the departure from the Gaussian behavior of the noise  $\eta(t)$ .  $\tau$  is the correlation time of non-Gaussian noise. The noise terms  $\epsilon(t)$  and the additive

noise term  $\xi(t)$  are Gaussian white noises with the following statistical properties:

$$\begin{aligned} \langle \epsilon(t) \rangle &= \langle \xi(t) \rangle = 0 \\ \langle \epsilon(t)\epsilon(t') \rangle &= 2D\delta(t-t') \\ \langle \xi(t)\xi(t') \rangle &= 2Q\delta(t-t') \\ \langle \epsilon(t)\xi(t') \rangle &= \langle \xi(t)\epsilon(t') \rangle = 2\lambda \sqrt{DQ}\delta(t-t') \end{aligned} \quad (6)$$

where  $D$  and  $Q$  are the noise intensities of the Gaussian noises  $\epsilon(t)$  and  $\xi(t)$ , and the parameter  $\lambda \in (-1, 1)$  is the cross-correlation strength between  $\epsilon(t)$  and  $\xi(t)$ .

When  $|q-1| \ll 1$  (both for  $q > 1$  and  $q < 1$ ), the non-Gaussian noise will only slightly depart from the Gaussian behavior, but will show some of the main trends of the  $q \neq 1$  region. Thus we can obtain the limit of  $\eta(t)$  being a Gaussian colored noise:

$$\begin{aligned} \frac{1}{\tau} \frac{d}{d\eta} V_q(\eta) &= \frac{\eta}{\tau} \left[ 1 + \frac{\tau(q-1)\eta^2}{D} \right]^{-1} \approx \\ &= \frac{\eta}{\tau} \left[ 1 + \frac{\tau(q-1)\langle \eta^2 \rangle}{D} \right]^{-1} = \frac{1}{\tau_{\text{eff}}} \eta(t) \end{aligned} \quad (7)$$

with effective noise correlation time

$$\tau_{\text{eff}} = \frac{2(2-q)\tau}{5-3q} \quad (8)$$

The distribution of  $\eta(t)$  can be written as:

$$\frac{d\eta(t)}{dt} = -\frac{1}{\tau_{\text{eff}}} \eta(t) + \frac{1}{\tau_{\text{eff}}} \epsilon'(t) \quad (9)$$

where  $\epsilon'(t)$  is Gaussian white noise with

$$\begin{aligned} \langle \epsilon'(t) \rangle &= 0 \\ \langle \epsilon'(t)\epsilon'(t') \rangle &= 2D_{\text{eff}}\delta(t-t') \end{aligned} \quad (10)$$

$D_{\text{eff}}$  represents effective noise intensity, given by

$$D_{\text{eff}} = \left[ \frac{2(2-q)}{5-3q} \right]^2 D \quad (11)$$

We assume  $\epsilon'(t)$  and  $\xi(t')$  satisfy the following statistical properties:

$$\begin{aligned} \langle \epsilon'(t)\xi(t') \rangle &= \langle \xi(t)\epsilon'(t') \rangle = \\ &= 2\lambda \sqrt{D_{\text{eff}}Q}\delta(t-t') \end{aligned} \quad (12)$$

Applying the UCNA theory<sup>[26-30]</sup> two-dimensional Markovian processes (1) and (9), we can obtain the following one-dimensional Markovian approximation<sup>[31]</sup>:

$$\begin{aligned} \frac{dx}{dt} &= \frac{h(x)}{c(\tau_{\text{eff}}, x)} + \frac{1}{c(\tau_{\text{eff}}, x)} \left[ g_1(x)\epsilon'(t) + \right. \\ &\quad \left. g_2(x)\xi(t) \right] \end{aligned} \quad (13)$$

in which

$$\begin{aligned}
 h(x) &= -\frac{dU(x)}{dx} + A\cos(\Omega t) \\
 g_1(x) &= x \\
 g_2(x) &= 1
 \end{aligned} \tag{14}$$

Thus

$$\begin{aligned}
 c(\tau_{\text{eff}}, x) &= 1 - \tau_{\text{eff}} \left[ h'(x) - \frac{g_1'(x)}{g_1(x)} h(x) \right] = \\
 &= 1 - \tau_{\text{eff}} \left\{ \left[ -\frac{dU(x)}{dx} + A\cos(\Omega t) \right]' - \right. \\
 &\quad \left. \frac{1}{x} \left[ -\frac{dU(x)}{dx} + A\cos(\Omega t) \right] \right\} = \\
 &= 1 + \tau_{\text{eff}} \left[ rx + 2bx^2 + \frac{A\cos(\Omega t)}{x} \right]
 \end{aligned} \tag{15}$$

The stochastic process (13) can be written as Stratonovich SDE

$$\frac{dx}{dt} = \frac{h(x)}{c(\tau_{\text{eff}}, x)} + \frac{1}{c(\tau_{\text{eff}}, x)} g(x) \Gamma(t) \tag{16}$$

with

$$g(x) = (D_{\text{eff}}x^2 + 2\lambda\sqrt{D_{\text{eff}}Q}x + Q)^{\frac{1}{2}} \tag{17}$$

in which  $\Gamma(t)$  is a Gaussian white noise. To simplify (16), let

$$\frac{dx}{dt} = \tilde{h}(x) + \tilde{g}(x) \Gamma(t) \tag{18}$$

with  $\tilde{h}(x) = \frac{h(x)}{c(\tau_{\text{eff}}, x)}$  and  $\tilde{g}(x) = \frac{g(x)}{c(\tau_{\text{eff}}, x)}$ . Then the Fokker-Planck (FPK) equation corresponding to Eq. (13)~(18) can be read as

$$\begin{aligned}
 \frac{dP(x,t)}{dt} &= -\frac{\partial}{\partial x} A(x)P(x,t) + \\
 &\quad \frac{\partial^2}{\partial x^2} B(x)P(x,t)
 \end{aligned} \tag{19}$$

with

$$\begin{aligned}
 A(x) &= \tilde{h}(x) + \tilde{g}(x)\tilde{g}'(x) \\
 B(x) &= \tilde{g}^2(x)
 \end{aligned} \tag{20}$$

According to the FPK equation (19), the steady-state probability density function  $P_{\text{st}}(x)$  can be obtained as follows:

$$\begin{aligned}
 P_{\text{st}}(x) &= N \frac{1}{\sqrt{B(x)}} \exp\left(\int \frac{A(x)}{B(x)} dx\right) = \\
 &= N \frac{1}{\sqrt{B(x)}} \exp\left(-\frac{\tilde{U}(x)}{D_{\text{eff}}}\right)
 \end{aligned} \tag{21}$$

in which  $N$  is a normalization constant.

When the external signal is not included, the generalized potential function  $\tilde{U}(x)$  has the following expression:

$$\tilde{U}(x) = \Phi_1(x) = D_{\text{eff}} \int \frac{U'(x)c(\tau_{\text{eff}}, x)}{g^2(x)} dx \tag{22}$$

When the external signal is included, the generalized potential function  $\tilde{U}(x)$  has the following expression (see Appendix B):

$$\begin{aligned}
 \tilde{U}(x) &= \Phi_2(x) = \\
 &= D_{\text{eff}} \int \frac{[U'(x) - A\cos(\Omega t)]c(\tau_{\text{eff}}, x)}{g^2(x)} dx
 \end{aligned} \tag{23}$$

### 3 SNR of the asymmetric bistable system and the influence of model parameters

Under the adiabatic approximation condition, the corresponding inverse transition rate  $W_{\pm}$  can be denoted as

$$\begin{cases}
 W_+ = \frac{|U''(x_{\text{un}})U''(x_{\text{s1}})|^{\frac{1}{2}}}{2\pi} \cdot \\
 \quad \exp\left[\frac{\tilde{U}(x_{\text{s1}}) - \tilde{U}(x_{\text{un}})}{D_{\text{eff}}}\right] \\
 W_- = \frac{|U''(x_{\text{un}})U''(x_{\text{s2}})|^{\frac{1}{2}}}{2\pi} \cdot \\
 \quad \exp\left[\frac{\tilde{U}(x_{\text{s2}}) - \tilde{U}(x_{\text{un}})}{D_{\text{eff}}}\right]
 \end{cases} \tag{24}$$

According to Eq. (24), the transition rate can be expanded by using Taylor series under small parameter conditions as

$$\begin{cases}
 W_+ = \omega_0^+ - \omega_1^+ \cdot A\cos(\Omega t) + o(A^2) \\
 W_- = \omega_0^- - \omega_1^- \cdot A\cos(\Omega t) + o(A^2)
 \end{cases} \tag{25}$$

The analytical expression for the signal-to-noise ratio (SNR) of the output signal can be obtained by both solving the FPK equation (19) and calculating the correlation function<sup>[22, 29]</sup>, which is given by

$$\text{SNR} = \frac{A^2\pi}{4\omega_0^+ \cdot \omega_0^-} \cdot \frac{(\omega_0^+ \cdot \omega_1^- + \omega_0^- \cdot \omega_1^+)^2}{\omega_0^+ + \omega_0^-} \tag{26}$$

where

$$\begin{aligned}
 \omega_0^+ &= W_+ \Big|_{A\cos(\Omega t)=0}, \omega_1^+ = \\
 &= -\frac{dW_+}{d[A\cos(\Omega t)]} \Big|_{A\cos(\Omega t)=0} \\
 \omega_0^- &= W_- \Big|_{A\cos(\Omega t)=0}, \omega_1^- = \\
 &= -\frac{dW_-}{d[A\cos(\Omega t)]} \Big|_{A\cos(\Omega t)=0}
 \end{aligned}$$

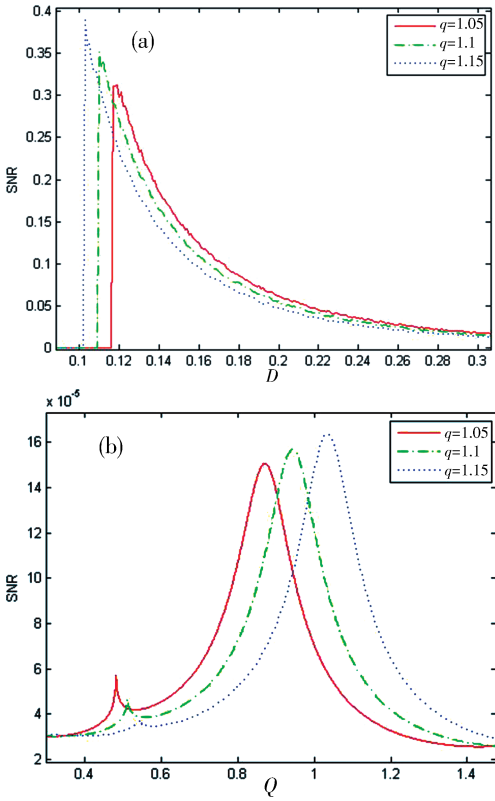


Fig. 2 The theoretical results of SNR are plotted as a function of the noise intensity when  $q$  varies: (a) characteristics of SNR versus  $D$  at  $Q=3.3$ ; (b) characteristics of SNR versus  $Q$  at  $D=3.3$

According to the expression of SNR, the influences of different parameters on the SR are discussed in Fig. 2~7.

Fig. 2 shows a curve of the SNR as a function of the non-Gaussian noise intensity  $D$  and Gaussian noise intensity  $Q$ , respectively, for different parameters of the non-Gaussian noise deviation parameter  $q$ . In Fig. 2(a), the SNR curve also produces a one-peak structure when noise intensity  $D$  is increased, which indicates that stochastic resonance phenomenon appears. The height of the peak is increased and the location of the peak is shifted to small value of  $D$  as deviation parameter  $q$  is increased. In Fig. 2(b), with the increase of  $Q$ , there are two peaks in the curves, and the right peak is always larger than the left peak. Firstly, from the figure, it is seen that there appears a weak peak in the SNR curve as  $Q$  is increased. Then the SNR curve is decreased, which is suppressed to a degree. As  $Q$  is continue in-

creased, there appears a pretty peak. It indicates that stochastic resonance phenomenon appears again. The height of the left peak is decreased while the right peak is increased, and the locations of both peaks are shifted to large value of  $Q$  as deviation parameter  $q$  is increased. It shows that as we choose variable values of  $q$ , the optimal value of noise intensity required is different when stochastic resonance phenomenon appears.

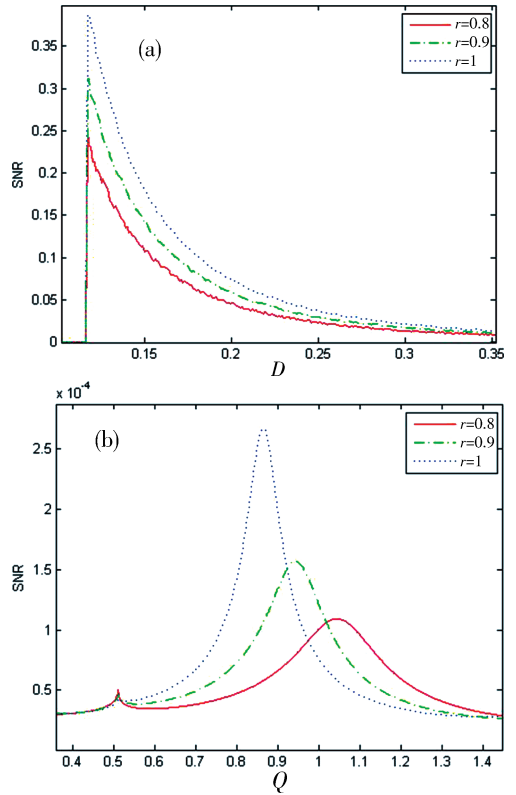


Fig. 3 The theoretical results of SNR are plotted as a function of the noise intensity when  $\tau$  varies: (a) characteristics of SNR versus  $D$  at  $Q=3.3$ ; (b) characteristics of SNR versus  $Q$  at  $D=3.3$

Fig. 3 shows a curve of the SNR as a function of the non-Gaussian noise intensity  $D$  and the Gaussian noise intensity  $Q$ , respectively, for different correlation times of the non-Gaussian noise  $\tau$ . In Fig. 3(a), the SNR curve produces a one-peak structure when noise intensity  $D$  is increased, which indicates that conventional stochastic resonance phenomenon appears. The peaks of curves increase as the correlation times of the non-Gaussian noise  $\tau$  increases. However, the position of the peak does not shift significant-

ly for different  $\tau$ . In Fig. 3(b), with the increase of  $Q$ , there are two peaks in the curves, and the right peak is always larger than the left peak. The height of the left peak is decreased while the right peak is increased, and the location of both peaks are shifted to small value of  $Q$  as correlation times of the non-Gaussian noise  $\tau$  is increased. It shows that as we choose variable values of  $\tau$ , the optimal value of noise intensity required is different when stochastic resonance phenomenon appears.

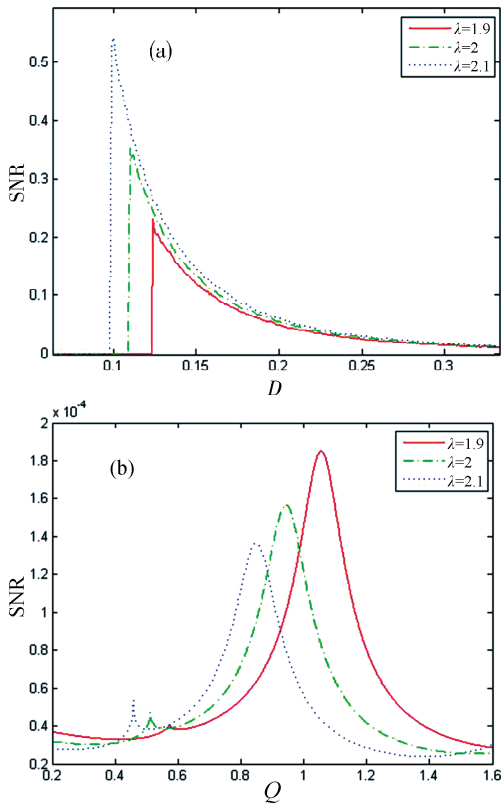


Fig. 4 The theoretical results of SNR are plotted as a function of the noise intensity when  $\lambda$  varies; (a) characteristics of SNR versus  $D$  at  $Q=3.3$ ; (b) characteristics of SNR versus  $Q$  at  $D=3.3$

Fig. 4 shows a curve of the SNR as a function of the non-Gaussian noise intensity  $D$  and the Gaussian noise intensity  $Q$ , respectively, for different cross-correlation strength  $\lambda$ . In Fig. 4(a), the SNR curve produces a one-peak structure when noise intensity  $D$  is increased. This is stochastic resonance. The peaks of curves increase as the cross-correlation strength  $\lambda$  increases. However, the location of the peak is shifted to small

value of  $D$  as parameter  $\lambda$  is increased. In Fig. 4 (b), there are two peaks in the curves with the increase of  $Q$ . The right peak is always larger than the left peak. The height of the left peak is increased while the right peak is decreased, and the locations of both peaks are shifted to small value of  $Q$  as cross-correlation strength  $\lambda$  is increased. It shows that as we choose variable values of  $\lambda$ , the optimal value of noise intensity required is different when stochastic resonance phenomenon appears. And we can find that there are different influences between Gaussian and non-Gaussian noise under cross-correlation strength  $\lambda$ .

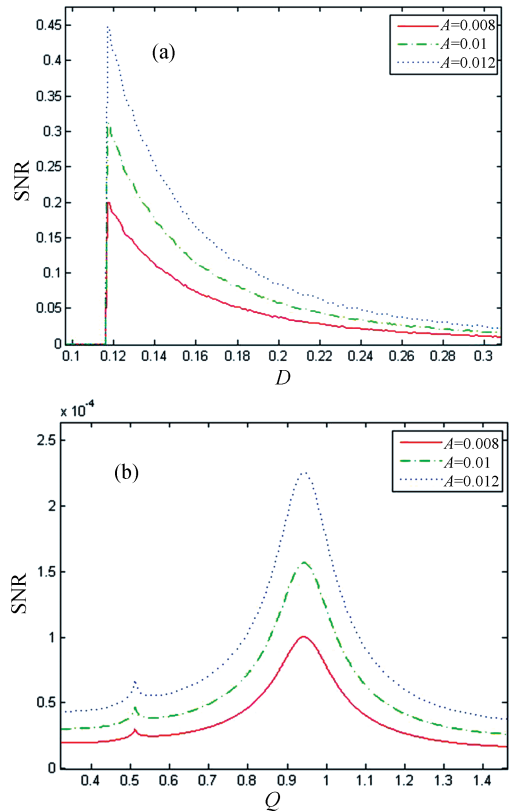


Fig. 5 The theoretical results of SNR are plotted as a function of the noise intensity when  $A$  varies; (a) characteristics of SNR versus  $D$  at  $Q=3.3$ ; (b) characteristics of SNR versus  $Q$  at  $D=3.3$

Fig. 5 shows a curve of the SNR as a function of the non-Gaussian noise intensity  $D$  and the Gaussian noise intensity  $Q$ , respectively, for different amplitudes  $A$  of periodic signal. In Fig. 5 (a), obviously, the SNR curve produces a one-peak structure when noise intensity  $D$  is increased, which indicates that conventional sto-

chastic resonance phenomenon appears. The height of the peak is increased as amplitudes  $A$  is increased. And the position of the peak does not shift significantly for different  $A$  which is reasonable in physical science. In Fig. 5(b), there are also two peaks in the curves with the increase of  $Q$  and the peaks of curves increase as  $A$  increases. Same as before, the position of the peak does not shift significantly for different  $A$ . It shows the system SNR is increased as amplitudes  $A$  is increased.

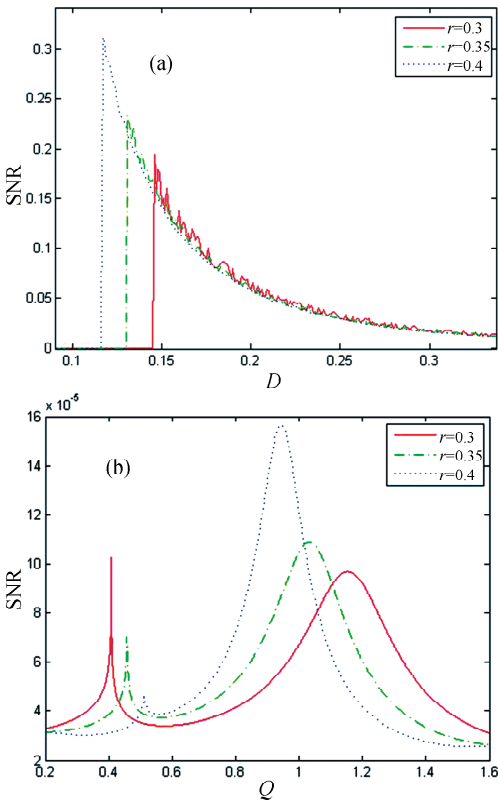


Fig. 6 The theoretical results of SNR are plotted as a function of the noise intensity when  $r$  varies: (a) characteristics of SNR versus  $D$  at  $Q=3.3$ ; (b) characteristics of SNR versus  $Q$  at  $D=3.3$

Fig. 6 shows a curve of the SNR as a function of the non-Gaussian noise intensity  $D$  and the Gaussian noise intensity  $Q$ , respectively, for different asymmetric coefficient  $r$ . In Fig. 6(a), the SNR curve also produces an obvious one-peak structure when noise intensity  $D$  is increased. This is conventional stochastic resonance. The peaks of curves increase as the asymmetric coefficient  $r$  increases. In Fig. 6(b), with the increase

of  $Q$ , there are two peaks in the curves, and the right peak is always larger than the left peak. The height of the left peak is decreased and the location of the left peak is shifted to large value of  $Q$  as asymmetric coefficient  $r$  is increased while the height of the right peak is increased and the location of the right peak is shifted to small value of  $Q$  as  $r$  is increased, which is different from the previous situation.

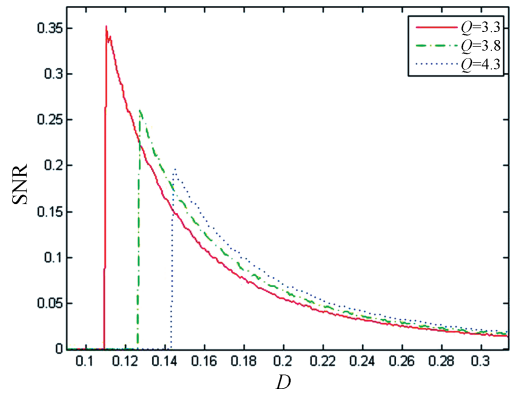


Fig. 7 The theoretical results of SNR are plotted as a function of the noise intensity  $D$  when  $Q$  varies

The SNR as a function of the non-Gaussian noise intensity  $D$  for different Gaussian noise intensities  $Q$  is described in Fig. 7. The SNR curve also produces an obvious one-peak structure when noise intensity  $D$  is increased. This is conventional stochastic resonance. The peaks of curves decrease as the Gaussian noise intensities  $Q$  increase. We can see that there is interaction between Gaussian and non-Gaussian noise.

## 4 Conclusions

In this paper, we studied the problem of stochastic resonance in an asymmetric nonlinear system driven by periodic signal and correlated noises for a multiplicative non-Gaussian noise and an additive Gaussian white noise in the case. The influence of different parameters on SNR is discussed, including non-Gaussian noise deviation parameter, correlation times of the non-Gaussian noise, cross-correlation strengths, amplitudes of periodic signal, asymmetric coefficient, and both Gaussian and non-Gaussian noise intensities.

From the simulation result, there is a differ-

ent result when the SNR is a function of the non-Gaussian noise intensity. Firstly, there appears a single peak in the SNR curves as a function of the non-Gaussian noise intensity while there are two peaks in the SNR curves with the increase of  $Q$ . Besides, as different parameters change, there are variation tendency of SNR. Especially, non-Gaussian noise deviation parameter  $q$  has different effect of the non-Gaussian noise on the location of the SNR peak from that of the Gaussian noise, and the cross-correlation strength  $\lambda$  has different effect of the non-Gaussian noise on the height of the SNR peak from that of the Gaussian noise.

### References:

- [1] Benzi R, Sutera A, Vulpiani A. The mechanism of stochastic resonance [J]. *J Phys A: Math Gen*, 1981, 14: 453.
- [2] Pesquera L, Rodriguez M A, Santos E. Path integrals for non-markovian processes [J]. *Phys Lett A*, 1983, 94: 287.
- [3] Colet P, Wio H S, San M M. Colored noise: a perspective from a path-integral formalism [J]. *Phys Rev A*, 1989, 39: 6094.
- [4] Presilla C, Marehesoni F, Gammaitoni L. Periodically time-modulated bistable systems: nonstationary statistical properties [J]. *Phys Rev A*, 1989, 40: 2105.
- [5] Jung P, Hanggi P. Stochastic nonlinear dynamics modulated by external periodic forces [J]. *Europhys Lett*, 1989, 8: 505.
- [6] Jung P, Hanggi P. Amplification of small signals via stochastic resonance [J]. *Phys Rev A*, 1991, 44: 8032.
- [7] Qiao Z J, Lei Y G, Lin J, *et al.* An adaptive unsaturated bistable stochastic resonance method and its application in mechanical fault diagnosis [J]. *Mech Syst Signal Pr*, 2017, 84: 731.
- [8] Zhao W, Wang L, Fan J. Theory and method for weak signal detection in engineering practice based on stochastic resonance [J]. *Int J Mod Phys B*, 2017, 31: 1750212.
- [9] Wang J, Han R, Wei X, *et al.* Weak signal detection and propagation in diluted feed-forward neural network with recurrent excitation and inhibition [J]. *Int J Mod Phys B*, 2016, 30: 1550253.
- [10] Guo Y F, Shen Y J, Tan J G. Stochastic resonance in a piecewise nonlinear model driven by multiplicative non-Gaussian noise and additive white noise [J]. *Commun Nonlinear Sci*, 2016, 38: 57.
- [11] Wio H S, Bouzat S. Stochastic resonance: the role of potential asymmetry and non Gaussian noises [J]. *Braz J Phys*, 1999, 29: 136.
- [12] Kwuimy C A K, Litak G, Nataraj C. Nonlinear analysis of energy harvesting systems with fractional order physical properties [J]. *Nonlinear Dynam*, 2015, 80: 491.
- [13] Tan D, Leng Y G, Fan S B, *et al.* Magnetic force of piezoelectric cantilever energy harvesting system with an externally applied magnetic field based on magnetizing current method [J]. *Acta Phys Sin: Ch Ed*, 2015, 64: 60502.
- [14] Inchiosa M E, Bulsara A R, Gammaitoni L. Higher-order resonant behavior in asymmetric nonlinear stochastic systems [J]. *Phys Rev E*, 1997, 55: 4049.
- [15] Gammaitoni L, Bulsara A R. Noise activated nonlinear dynamic sensors [J]. *Phys Rev Lett*, 2002, 88: 230601.
- [16] Zhou B C, Lin D D. Stochastic resonance in an asymmetric bistable system driven by multiplicative and additive trichotomous noises [J]. *Chin J Phys*, 2017, 55: 1078.
- [17] Jiao S B, Yang R, Zhang Q, *et al.* Stochastic resonance of asymmetric bistable system with alpha stable noise [J]. *Acta Phys Sin: Ch Ed*, 2015, 64: 20502.
- [18] Wiesenfeld K, Pierson D, Pantazelou E, *et al.* Stochastic resonance on a circle [J]. *Phys Rev Lett*, 1994, 72: 2125.
- [19] Nozaki D, Mar D J, Grigg P, *et al.* Politics-Oprah style millions watch as gore gets personal on talk show [J]. *Phys Rev Lett*, 1999, 82: 2402.
- [20] Fuentes M A, Toral R, Wio H S. Enhancement of stochastic resonance: the role of non Gaussian noises [J]. *Physica A*, 2001, 295: 114.
- [21] Wio H S, Toral R. Effect of non-Gaussian noise sources in a noise-induced transition [J]. *Physica D*, 2004, 193: 161.
- [22] Fuentes M A, Wio H S, Toral R. Effective Markovian approximation for non-Gaussian noises: a path integral approach [J]. *Physica A*, 2002, 303: 91.
- [23] Guo Y F, Xi B, Wei F, *et al.* Stochastic resonance in FitzHugh - Nagumo neural system driven by correlated non-Gaussian noise and Gaussian noise

- [J]. *Int J Mod Phys B*, 2017, 31: 1750264.
- [24] Shi P M, Li Q, Han D Y. Stochastic resonance and MFPT in an asymmetric bistable system driven by correlated multiplicative colored noise and additive whitenoise [J]. *Int J Mod Phys B*, 2017, 31: 1750113.
- [25] Nikitin A, Stocks N G, Bulsara A R. Asymmetric bistable systems subject to periodic and stochastic resonance forcing in the strongly nonlinear regime: switching time distributions [J]. *Phys Rev E*, 2003, 68: 016103.
- [26] Jung P, Hänggi P. Dynamical systems: a unified colored-noise approximation [J]. *Phys Rev A*, 1987, 35: 4464.
- [27] Wu D J, Cao L, Ke S Z. Bistable kinetic model driven by correlated noises: steady-state analysis [J]. *Phys Rev E*, 1994, 50: 2496.
- [28] Cao L, Wu D J, Ke S Z. Bistable kinetic model driven by correlated noises: unified colored-noise approximation [J]. *Phys Rev E*, 1995, 52: 3228.
- [29] Jia Y, Zheng X P, Hu X M, *et al.* Effects of colored noise on stochastic resonance in a bistable system subject to multiplicative and additive noise [J]. *Phys Rev E*, 2001, 63: 031107.
- [30] Wang J, Cao L, Wu D J. Effect on the mean first passage time in symmetrical bistable systems by cross-correlation between noises [J]. *Phys Lett A*, 2003, 308: 23.
- [31] Wang F Z, Tan Z A, Dai S Y, *et al.* Recent advances in planar heterojunction organic-inorganic hybrid perovskite solar cells [J]. *Acta Phys Sin; Ch Ed*, 2015, 64: 038401.

**引用本文格式:**

中文: 范泽宁, 李鹏飞, 陶原野, 等. 相关噪声驱动下一种特殊非对称非线性系统的随机共振研究[J]. *四川大学学报: 自然科学版*, 2020, 57: 927.

英文: Fan Z N, Li P F, Tao Y Y, *et al.* Stochastic resonance in a special type of asymmetric nonlinear system driven by correlated noise [J]. *J Sichuan Univ; Nat Sci Ed*, 2020, 57: 927.